Side-chain structure and dynamics at the lipid-protein interface: Val1 of the gramicidin A channel

ARTICLE *in* BIOPHYSICAL JOURNAL · JUNE 1994

Impact Factor: 3.97 · DOI: 10.1016/S0006-3495(94)80928-2 · Source: PubMed

2 AUTHORS, INCLUDING:

Timothy Cross
Florida State University
251 PUBLICATIONS **9,344** CITATIONS

Side-Chain Structure and Dynamics at the Lipid-Protein Interface: Val_1 of the Gramicidin A Channel

K.-C. Lee and T. A. Cross
Department of Chemistry, Institute of Molecular Biophysics, and National High Magnetic Field Laboratory, Florida State University, Tallahassee, Florida 32306 USA

ABSTRACT High resolution dynamics and structural information has been resolved from ^2H solid-state NMR spectra of the Val-1 side-chain of the gramicidin channel in a lipid bilayer. Both powder pattern lineshapes and spectra from uniformly aligned samples of gramicidin in lipid bilayers have been analyzed to achieve a fully consistant interpretation of the data. Torsional motions about the $C_\alpha C_\beta$ axis (χ_1) are shown to be three-state jumps in which the occupancy of the states is given by the ratio, 75:15:10 for the χ_1 angles of 184°:304°:64°. The dominant conformer is also the most common conformation observed for valines in well defined protein structures. The distribution of conformational substates that represents the χ_1 dynamics appears to be largely independent of the lipid phase transition and the hydration of the sample. However, there is evidence that the residence time between jumps is dependent on the lipid phase transition. Although this time is shown to be approximately 1 μs below the phase transition temperature, it is in the fast exchange limit above the transition temperature.

INTRODUCTION

A long-standing goal in membrane biophysics has been to characterize the influences of lipid on protein, and protein on lipid in model membranes. Solid-state NMR has long been recognized as having the potential to contribute in this arena; however, there have been and continue to be numerous complications. One of the most challenging is the separation of structural and dynamic influences on the solid-state NMR spectra. Here, characterizations are achieved for the dynamics and conformation of the Val-1 side-chain in the gramicidin dimer that forms a channel in lipid bilayers. By using a combination of unoriented and oriented bilayer preparations, above and below the phase transition of the lipid, it has been possible to separate these influences and to achieve a quantitative description of the χ_1 torsional dynamics and conformational states for this side-chain.

Gramicidin A is a hydrophobic linear peptide containing 15 alternating D and L amino acid residues, and termini are blocked such that the peptide has no formal charges. The primary sequence is HCO-(L)Val_1-Gly_2-(L)Ala_3-(D)Leu_4-(L)Ala_5-(D)Val_6-(L)Val_7-(D)Val_8-(L)Trp_9-(D)Leu_{10}-(L)Trp_{11}-(D)Leu_{12}-(L)Trp_{13}-(D)Leu_{14}-(L)Trp_{15}-NHC_2H_4OH. As an amino-terminus to amino-terminus dimer this peptide forms a monovalent cation selective channel. Models of the folding motif have been extant for many years (Wallace, 1990; Anderson et al., 1992; Killian, 1992), and recently the backbone structure has been solved in a lipid environment (Ketchem et al., 1993). The motif is a helix with 6.3 residues per turn forming a 4-Å pore through which a single file of water molecules and cations can pass. How the peptide facilitates cation transport is not known, but local motions in the backbone with substantial amplitudes and nanosecond frequencies suggest that dynamic and kinetic processes are occuring on the same timescale (North and Cross, 1993; North, 1993). To achieve local motional frequencies on such a slow timescale, the motions are likely to be highly correlated. The dynamics of the backbone may be correlated with the side-chains and may be modulated further by the lipids. It is known that lipids can modulate the conductance of the gramicidin channel.

The analysis of chemical shift or ^2H quadrupolar powder patterns is the most common approach for characterizing dynamic modes by solid-state NMR. Molecular motions average the nuclear spin interaction tensors, thereby changing the shape and reducing the width of the spectral lineshape. Spectra of samples that have been aligned uniformly with respect to the magnetic field are also affected by these motions. The observed frequencies reflect the orientation of the spin interaction with respect to the field, but a quantitative interpretation of such orientational or structural constraints requires a characterization of the motionally averaged spin interaction tensors. Previous efforts (Killian et al., 1992) to characterize the dynamics and conformation of the Val-1 site in gramicidin did not have the dynamic insight afforded by the temperature-dependent powder pattern analysis for the valine methyl groups.

MATERIALS AND METHODS

Sample preparation

D_8 L-Valine was obtained from Cambridge Isotope Lab (Cambridge, MA). Formyl-L-Valine was prepared as described previously (Mai et al., 1993). The solid phase peptide synthesis (0.5 mmol) was performed on an Applied Biosystems Inc., model 430A peptide synthesizer using Fmoc chemistry with hydroxyl-methyl resin as described in Fields et al. (1988, 1989). For efficient utilization of the label, 0.5 mmol of formyl-L-Val-d_8 was coupled followed by recoupling with 1.0 mmol of formyl-L-Val to complete the

Received for publication 27 September 1993 and in final form 31 January 1994.

Address reprint requests to Timothy A. Cross, Department of Chemistry, National High Magnetic Field Laboratory, Florida State University, 1800 East Paul Dirac Drive, Tallahassee, FL 32306-3016. Tel.: 904-644-0917; Fax: 904-644-0867; E-mail: cross@magnet.fsu.edu.

0006-3495/94/05/1380/08 $2.00

synthesis. Ethanolamine was used to cleave the peptide from the resin. Approximately 99% purity was obtained in this crude extract when checked with reverse phase HPLC at 280 nm.

A powder sample of gramicidin and lipid was prepared by mixing about 50 mg of Val_1-d_8 gramicidin with 145 mg of dimyristoylphosphatidylcholine (DMPC) (1:8 molar ratio) in 95% MeOH/H_2O solution. Water used in all sample preparations was deuterium-depleted. This sample was dried thoroughly under vacuum. The hydrated unoriented sample was prepared by adding 40% by weight water to the powder sample. It was then allowed to hydrate at 45° (gel to liquid crystal phase transition is 28°) for at least 2 weeks. Oriented samples were prepared by mixing 30 mg of Val_1-d_8 gramicidin A with 86 mg of DMPC in 95% MeOH/H_2O solution. The solution was stored in a freezer overnight. After thawing, the solution was applied in equal aliquots to 20 glass plates (20x5 mm; 4 mm of length was used for spacers between the cover slips). The samples were first dried in a desiccator and then placed under vacuum overnight to remove any residual solvent. The glass plates were then stacked in a square glass tube and hydrated with 40% by weight water. After sealing the square tube, the sample was stored in the incubator for more than 2 weeks at 45°C.

^{2}H NMR experiment and simulations

The ^{2}H NMR spectra were recorded using a homebuilt Chemagnetics data acquisition system with a 400/89 Oxford Instruments (Oxford, England) wide-bore magnet. The homebuilt single frequency ^{2}H probe was tuned to 61.5 MHz with a horizontal solenoid coil. A top-loading variable temperature stack was implemented for accurate temperature control in the experiments. Dual sensors for temperature measurement were located around the sample coil for determining the inlet and outlet gas temperature. Approximately 30 min was allowed for achieving thermal equilibrium. A 1 MHz sweep width, 2.8 μs 90° pulse width, 30 μs echo delay, and an 8 step phase cycling routine was employed for acquisition with the standard quadrupole pulse sequence (Davis et al., 1976). The recycle delay was 0.7 s for all samples except 30 s for the valine-d_8 powder sample.

The simulated spectra were calculated using single precision calculations in the Fortran program, MXQET (Greenfield et al., 1987) on a Silicon Graphics Personal Iris 4D/25TG workstation. All simulated spectra were corrected for finite pulse length and echo delay. The Val_1 side-chain dynamic and structural results were calculated and displayed using the annealed gramicidin backbone structure (Ketchem et al., 1993) with Insight II Biosym software.

Spectral simulations

The quadrupole interaction for the spin 1, ^{2}H nucleus has two orientation-dependent resonance frequencies in the magnetic field. The splitting between these two resonances can be written as

$$\begin{aligned} \Delta\nu_{obs} &= 2\delta(3\cos^4\theta - 1 - \eta\sin^2\theta\cos 2\phi) \\ \delta &= 3/8(e^2qQ/h) \\ \eta &= (\nu_{yy} - \nu_{xx})/\nu_{zz} \qquad 1 \geq |\eta| \geq 0 \\ |\nu_{zz}| &\geq |\nu_{xx}| \geq |\nu_{yy}|, \end{aligned} \tag{1}$$

where ν_{ii} are the elements of the electric field gradient tensor, and θ and ϕ are the polar angles of the magnetic field vector in the principal axis system. The static quadrupole coupling constant (e^2qQ/h) is 171 ± 5 kHz (Keniry et al., 1984), and the asymmetry parameter, η, is approximately 0.05 for aliphatic CD bonds and will be further approximated here as 0. Consequently, in the absence of motions the frequency of the quadrupole splitting will be only dependent on θ. Rapid axial rotation of the methyl group (about the $C_\beta C_\gamma$ axis) or three-state tetrahedral jumps with equal occupancy in each state maintains the axial symmetry of the tensor, but averages the quadrupole coupling constant by a factor of 3 in the molecular symmetry axis frame, assuming ideal tetrahedral geometry for the motional frame. Similarly, rapid axial rotation about the $C_\alpha C_\beta$ axis or three-state tetrahedral jumps with equal occupancy in each state continues to maintain the axial symmetry and further averages the tensor by a factor of 3 in this intermediate motional frame of reference (SYM), which reflects symmetric averaging of the tensor. However, if the three states are unequally populated the tensor becomes asymmetric and the matrix presents off-diagonal terms. Diagonalization of this matrix yields an asymmetric tensor with averaged elements and a nonzero value for η in the A3S (asymmetric three-state averaging) frame of reference. In an extreme example of this motion where two states are equally populated and the third is not populated, the asymmetry parameter becomes unity in this A2S (asymmetric two-state averaging) frame of reference.

For each frame of reference a unique motional axis, ν_{zz} can be defined for each unique deuterium nucleus (Fig. 1). For equal populations in a three-state jump the axis, ν_{zz}(SYM) is defined similarly to that for the methyl rotor; the axis makes an angle of 70° with respect to each of the $C_\beta C_{\gamma 1}$, $C_\beta C_{\gamma 2}$, and $C_\beta D$ bonds if ideal tetrahedral geometry prevails. For equal populations in a two-state jump the motional axis, ν_{zz}(A2S) is the bisector of the angle formed by the two conformers, thereby making an angle of 54.7° with respect to each conformer state, again assuming ideal tetrahedral geometry. For the third situation in which unequal populations exist for each of three states, the motional axis, ν_{zz}(A3S) is shifted toward the dominant conformer and it is dependent upon the precise distribution of conformers among the tetrahedral sites.

RESULTS AND DISCUSSION

Lineshape analysis

Spectra of valine methyl deuterons in crystalline samples have been analyzed previously (Beshah and Griffin, 1989). The 38-kHz splitting for the perpendicular components of the powder pattern is only slightly smaller than the results from alanine methyl deuterons (Kinsey et al., 1981; Keniry et al., 1984). Consequently, the valine side-chain group shows no additional large amplitude motion, but only an incremental increase in high frequency librational amplitude. Fig. 2 shows the L-valine-d_8 dry crystalline ^{2}H NMR powder pattern spectrum. The outer splitting can be assigned to C_α and C_β deuterons. Because of the relatively rigid structure for these latter deuterons and the long T_1 relaxation times, a 30 s recycle delay was used to obtain this spectrum. The strong intensity for the inner $\Delta\nu_\perp$ splitting has been averaged by methyl, $C_\beta C_\gamma$, rotation. The simulated spectrum of this powder pattern in Fig. 2 *B* was obtained by using a librationally

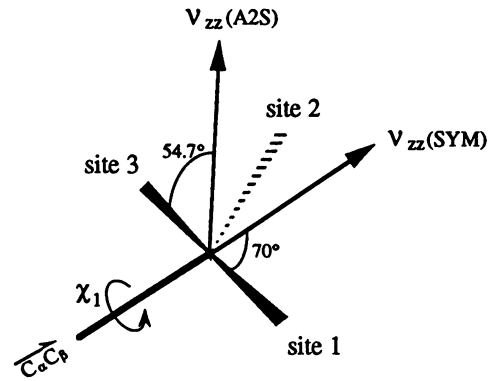

FIGURE 1 The molecular reference frame for motions about the χ_1 torsion angle in the valine side-chain. Free rotation about the $C_\alpha C_\beta$ bond or a three-state jump motion between tetrahedral sites with equal probability for each rotameric state will lead to a motional axis, ν_{zz}(SYM). A jump motion between two of the rotameric states leads to a motional axis, ν_{zz}(A2S), as shown when populations for the sites are equal.

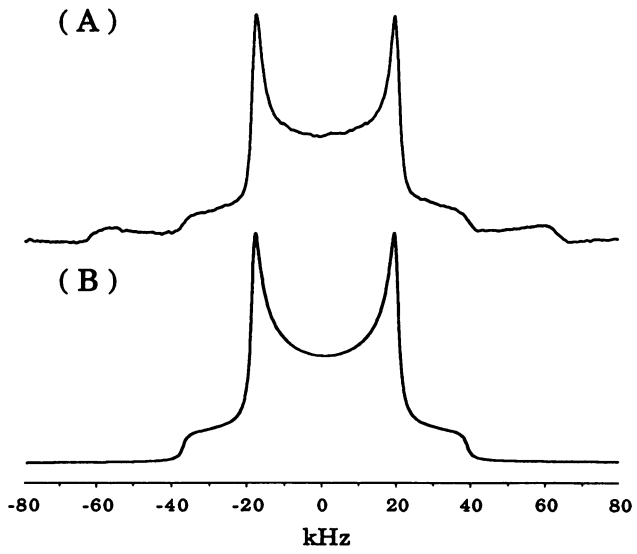

FIGURE 2 Experimental and Calculated ^{2}H NMR powder pattern spectra of a d_8-L-valine crystalline sample. (*A*) Experimental spectrum obtained with 32 acquisitions and a 30 s recycle delay using the quadrupole echo pulse sequence. (*B*) Simulated spectrum of the two methyl-d_3 sites using a three-state jump model with equal probability in the fast exchange limit between tetrahedral sites.

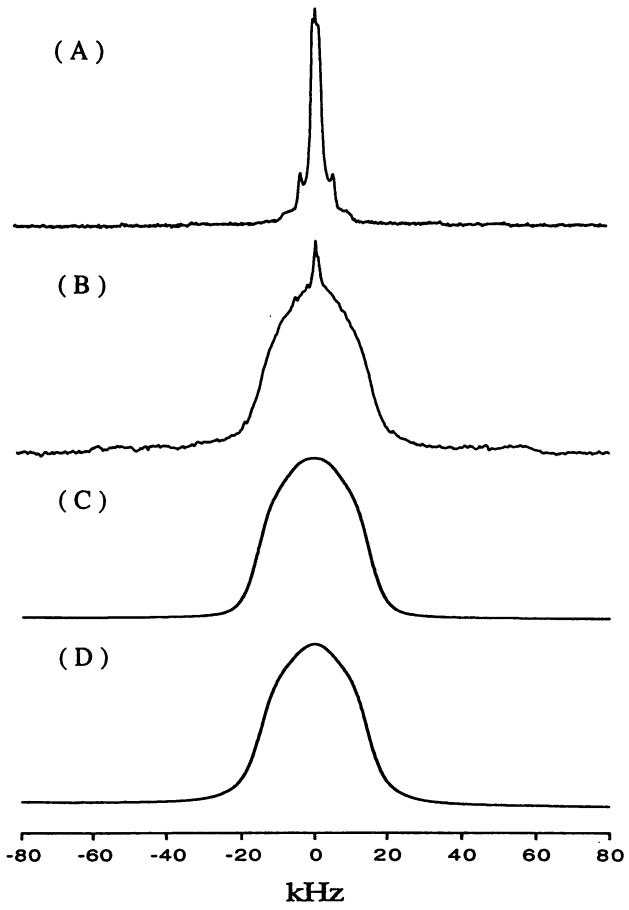

FIGURE 3 ^{2}H NMR powder pattern spectra of d_8-L-Val_1 gramicidin A in DMPC bilayers hydrated with 40% by weight deuterium-depleted water. (*A*) Experimental spectrum obtained with 20k acquisitions and a 1.0 s recycle delay using the quadrupole echo pulse sequence at 36°C. (*B*) Experimental spectrum obtained as in *A* with 50k acquisitions at 5°C. (*C*) Simulated spectrum of the deuterated methyl sites using a two-state jump model between tetrahedral sites with a 40 kHz qcc, a residence time between jumps of 1 μs, and an occupancy ratio of 70:30 for the two states. (*D*) Simulated spectrum for a three-state jump model using a 46 kHz qcc, a residence time between jumps of 1.5 μs, and an occupancy ratio of 75:15:10 for the three states.

averaged quadrupole coupling constant, qcc, of 155 kHz corresponding to a $\Delta\nu_\perp$ value of 38.8 kHz for the methyl deuterons. In macromolecules, additional averaging of the valine-d_8 interaction has been observed. Two-state jumps about the $C_\alpha C_\beta$ axis among tetrahedral sites (Fig. 1) have been reported in different polymers (Batchelder et al., 1982; Colnago et al., 1987; Leo et al., 1987; Keniry et al., 1983). This two-state jump model has also been demonstrated for situations where the occupancy of each state is unequal (Huang et al., 1980; Lee et al., 1986).

Fig. 3 *A* shows the ^{2}H powder pattern spectrum of Val_1-d_8 gramicidin A in hydrated DMPC bilayers at 36°C. The resonances for $C_\alpha D$ and $C_\beta D$ have very short T_{2e} relaxation times and, hence, very poor sensitivity under these spectral conditions. The spectrum shows the superposition of powder patterns for the two different methyl groups. The averaging of the quadrupole coupling constant results from multiple motions. When the gramicidin A channel conformation is formed in DMPC bilayers, global motion of the peptide about the channel axis parallel with the bilayer normal vector takes place (Fields et al., 1988). This motion has a correlation time of 36 μs at 36°C (Lee et al., 1993). Thus, the global motion of the peptide, the motion of the methyl group about the $C_\beta C_\gamma$ axis, and librational motions (Nicholson et al., 1991) all contribute to the averaging of the electric field gradient tensors, resulting in a narrow powder lineshape. The correlation time for the global motion can be increased to greater than 1.3 s at 5°C, which is below the gel to liquid crystalline phase transition temperature of the lipid sample (Lee et al., 1993). When the Val_1-d_8 gramicidin A hydrated sample temperature is so lowered, a broad and rounded lineshape is observed (Fig. 3 *B*). If there was only fast methyl reorientation and a small amplitude librational motion, a Pake powder pattern would be expected. The only realistic large-amplitude motion that could cause this lineshape for the Val_1 side chain site is motion about the $C_\alpha C_\beta$ bond as observed in other macromolecular samples described above.

Two approaches were taken for the simulation of this 5°C powder pattern. A two-state jump with unequal occupancies (70:30 ratio) and an average residence time of 1 μs was used for Fig. 3 *C*. This simulation required additional librational averaging of the quadrupole coupling constant to 143 kHz (see Table 1), resulting in a $\Delta\nu_\perp$ value of 30 kHz after the two-state jump motion. Fig. 3 *D* shows the three-state jump simulation using an unequal occupancy ratio of 75:15:10 and a 1.5 μs average occupancy time. Here the librationally averaged quadrupole coupling constant is 155 kHz, resulting in a $\Delta\nu_\perp$ of 34.5 kHz after the three-state jump motion. Both of these simulations provide good fits to the experimental

TABLE 1 Effective qcc averaged by three levels of local motion, derived from spectral simulations

	Static	Librational avg.	χ_1 avg.	χ_2 avg.
	kHz	kHz	kHz	kHz
$C_\alpha D$	171	155		
$C_\beta D$				
2 states (70:30)	171	143	120	
3 states (75:15:10)	171	155	138	
$C_\gamma D$				
2 states (70:30)	171	143	120	40
3 states (75:15:10)	171	155	138	46

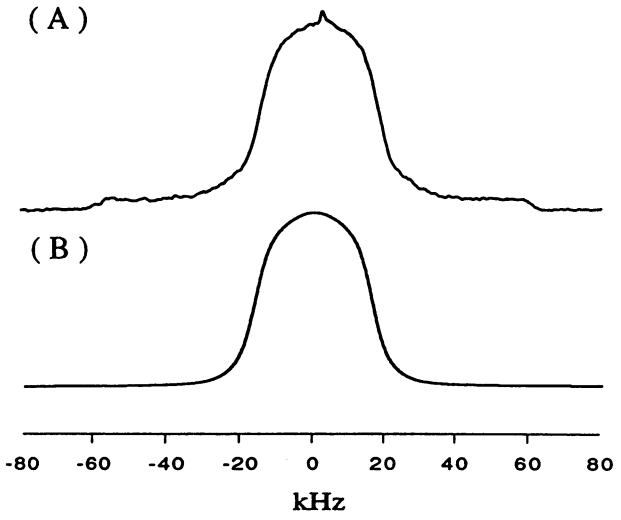

FIGURE 4 ^2H NMR powder pattern spectra of d_8-L-Val_1 gramicidin A in DMPC bilayers. (*A*) Experimental spectrum of a lyophilized sample that had been hydrated previously to ensure bilayer and channel formation. 20k acquisitions and 0.7 s recycle delay were used in the quadrupole echo pulse sequence. (*B*) Simulated spectrum using a three-state jump model with a 48 kHz qcc, a residence time between jumps of 1.5 μs, and an occupancy ratio of 75:20:5 for the three states.

lineshape. The theoretical value of the averaged quadrupole coupling constant for a nonlibrating methyl rotor is 57 kHz (static qcc = 171 kHz). For the two-state model the quadrupole coupling constant has been reduced by about 16%, whereas the three-state model required a 10% reduction due to the librational motion. A 5–10% reduction of the quadrupole coupling constant for librational averaging has been used previously (Prosser et al., 1991). However, librational amplitudes may increase for each torsion angle away from the polypeptide backbone. The slightly better fit between experimental and simulated lineshapes for the three-state model and the reduced dependence on librational averaging suggests that this model, which is a generalized two-state model, should be used here. For the rest of the analysis in this report we have used the three-state model with unequal occupancy and assumed ideal tetrahedral geometry. This latter assumption has been adopted to reduce the number of variables used for fitting the experimental results.

Furthermore, a lyophilized powder sample of Val_1-d_8 gramicidin A shows a similar broad but somewhat flatter powder lineshape as shown in Fig. 4 *A*. This spectrum can also be simulated by a three-state jump between states with an unequal occupancy ratio of 75:20:5 (Fig. 4 *B*). These occupancies represent a slight difference from that described above for hydrated bilayers below the gel to liquid crystalline phase transition temperature. A slight increase in the steric hindrance about the χ_1 angle could result from reduced solvent induced dynamics, or a possible conformational change as a result of lyophilization and solvent elimination.

The residence time in these conformational substates between jumps borders on the intermediate time frame. For the lyophilized and hydrated 5°C powder patterns, residence times of 1 and 1.5 μs have been used, respectively, for the simulations. Simulations with shorter residence times yield substantially sharper discontinuities. Above the phase transition temperature, the powder pattern of a hydrated sample shows very sharp discontinuities, and the spectra of oriented samples show sharp resonances, indicative of the fast exchange limit. Therefore, it is anticipated that the residence times between jumps will be significantly shorter when the samples are above the phase transition temperature.

The geometry of the motion axis

For the occupancy ratio of 75:15:10, Fig. 5 shows that the motional axis, ν_{zz}(A3S), makes an angle of 60° with respect to the $C_\alpha C_\beta$ bond axis, whereas the $C_\beta C_\gamma$ and $C_\beta D$ bond axes form 70° angles with the $C_\alpha C_\beta$ axis and ν_{zz}(SYM). Furthermore, because the two minor populations differ, the ν_{zz}(A3S) axis is not aligned with the dominant state, but is rotated toward the greater of the two minor populations by 4°. The

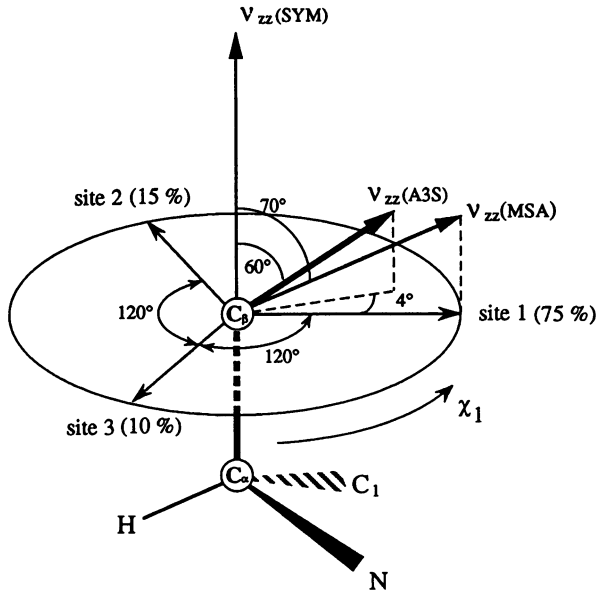

FIGURE 5 The geometry for three-state tetrahedral jumps about the χ_1 angle. The ν_{zz}(MSA) motional axis is equivalent to the $C_\beta D$ or $C_\beta C_\gamma$ axes. The ν_{zz}(SYM) axis is as defined in Fig. 1, and the ν_{zz}(A3S) axis is for the three-state jump in which the occupancy of the three states has the ratio of 75:15:10.

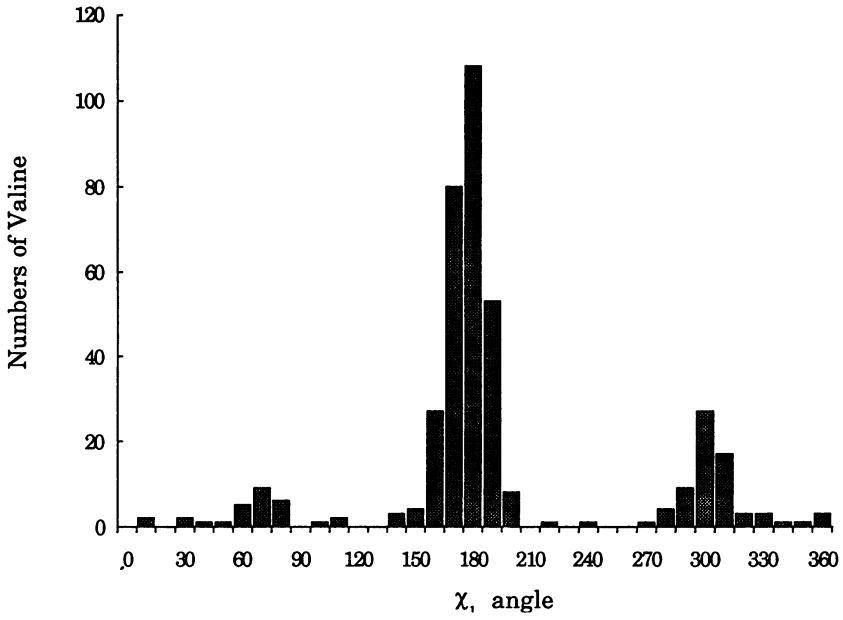

FIGURE 6 A statistical analysis of valine χ_1 angles obtained from x-ray crystallographic results of 20 proteins refined to less than 1.5-Å resolution.

projection of the $C_\beta C_\gamma$ and $C_\beta D$ bond axes onto a plane normal to the $C_\alpha C_\beta$ bond shows the assumed ideal rotational angle of 120° for this motional model. The identification of the jump states with specific χ_1 angles is dependent on structural information. The statistical analysis of the χ_1 distribution among the valine residues from the protein structures in the Brookhaven Data Bank determined at 1.5 Å resolution or less is shown in Fig. 6. The dominant conformer has a χ_1 value of approximately 180° and the second most common conformer a value of approximately 300°. In Fig. 5, if site 1 is arbitrarily chosen as the dominant conformer, then site 2 (site 1 + 120°) is the second most common conformer and site 3 (site 1 − 120°) is the least populated of the conformer states. Based on the use of this distribution of conformers in the data bank, the orientation of the ν_{zz}(A3S) axis is rotated by 4° in the positive χ_1 direction with respect to ν_{zz}(MSA) and the bond vector.

χ_1 Angle determination

The powder pattern analysis above has generated a detailed model for the molecular motions in which the side-chain jumps among three rotameric states, and among these states a dominant conformer exists. To determine the χ_1 angle for this dominant conformer, it is necessary to analyze the room temperature spectra of hydrated bilayer preparations. Furthermore, it is essential to take into account the constraints defined by the backbone structure that has been published recently (Ketchem et al., 1993).

Spectra of uniformly oriented gramicidin A are shown in Fig. 7. The observed splitting represents $\Delta\nu_\parallel$ of the motionally averaged quadrupole interactions for which both global and local motions are important. The spectral assignments can be made as follows for the 36°C spectrum. The orientation of the $C_\alpha D$ bond from the backbone structural analysis is known to be approximately 11° and is readily assigned, therefore, to the 205-kHz splitting by using a librationally averaged qcc of 155 kHz (Table 1). The remaining large splitting, 133 kHz, must be due to the $C_\beta D$ because the

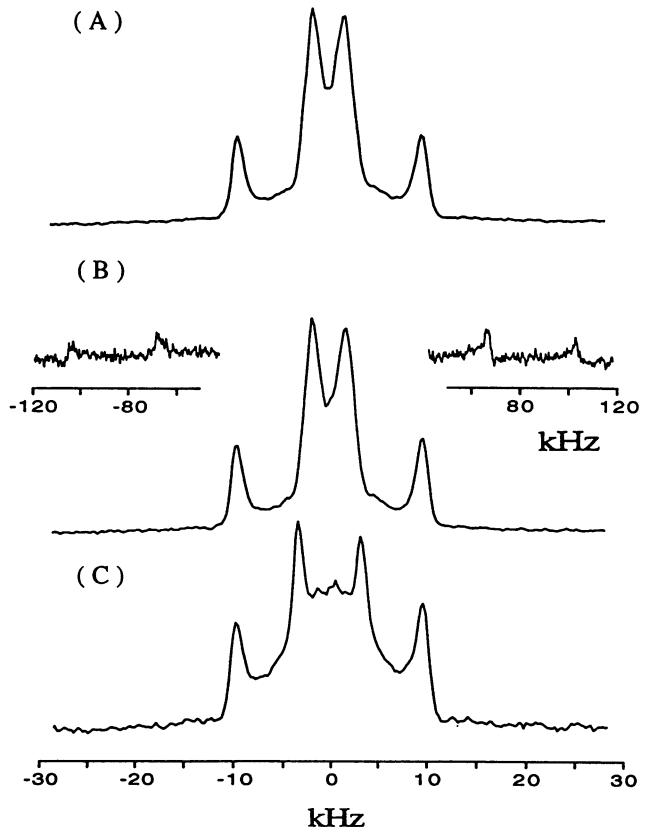

FIGURE 7 Experimental ^2H NMR spectra of oriented preparations of d_8-L-Val_1 gramicidin A in hydrated DMPC bilayers. The channel axis was aligned with the magnetic field direction. 20k acquisitions and 0.7 s recycle delay were used in the quadrupole echo pulse sequence. The temperature was controlled at (*A*) 52°C, (*B*) 36°C, and (*C*) 22°C.

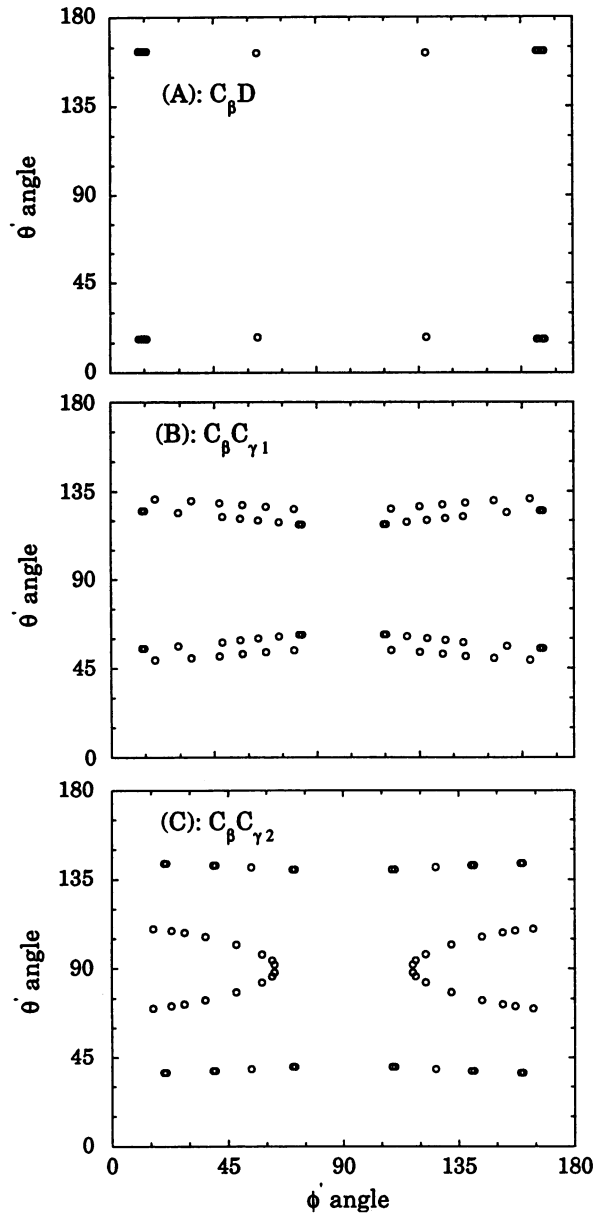

FIGURE 8 Graphs of the polar angles θ' and ϕ' (which orient the ν_{zz}(A3S) axis with respect to the magnetic field) that are consistent with the quadrupolar splittings in the d_8-L-Val_1 gramicidin A spectra at 36°C are shown. (*A*) The quadrupolar splitting for $C_\beta D$ is 133.4 kHz, and there are only two θ' solutions. (*B*) The quadrupolar splitting for $C_\beta C_{\gamma 1}$ is 3.8 kHz, and there are two relatively narrow ranges for θ' angles between 49° and 63° and between 117° and 131°. (*C*) The quadrupolar splitting for $C_\beta C_{\gamma 2}$ is 19.1 kHz, and the range of θ' angles is broad.

methyl deuterons will be averaged to a greater extent. The two intense quadrupole splittings, 19.1 and 3.8 kHz, derive from the d_3-methyl sites that are averaged by global motions, χ_1 jump motions, χ_2 methyl rotation, and small amplitude librational motions.

The quadrupole splitting of the $C_\beta D$ can also be used to constrain the possible orientation for this bond with respect to the magnetic field. The polar angles θ' and ϕ' define the orientation of the magnetic field direction in the A3S frame of reference (three-state jump with occupancies of 75:15:10). Although the channel has an axial global motion, the oriented samples are aligned such that this motional axis is parallel with respect to the magnetic field and, consequently, it does not average the Z_{lab} components of the tensor. Solutions for these angles from Eq. 1 are plotted in Fig. 8 *A*, and are consistent with the $C_\beta D$ quadrupole splitting in which qcc is reduced from a static value of 171 kHz to a librationally averaged value to 155 kHz and $\eta = 0.258$. The θ' angle for the averaged $C_\beta D$ axis has two solutions, 162° and 18°. The $C_\alpha C_\beta$ bond orientation with respect to the channel axis and the magnetic field is known for the Val_1 residue from the published backbone structure of the channel to be approximately 100° (Ketchem et al., 1993). As seen in Fig. 9 where the $C_\alpha C_\beta$ bond orientation is taken as 105°, the only θ' angle that is consistent with this additional constraint and with the tetrahedral geometry for the C_β site is 162°.

To determine the χ_1 torsion angle it is necessary to convert from a consideration of the motional axis for $C_\beta D$ to the bond orientation in its dominant and minor conformer states. The $C_\beta D$ orientation is highly restricted by the large quadrupolar splitting for this site. In fact, the dominant conformer must be in the *trans* (approximately 180°) conformation. In Fig. 9 θ' is calculated as a function of the rotation angle for the $C_\beta D$ ν_{zz}(A3S) axis about the $C_\alpha C_\beta$ bond. This angle differs from χ_1, which reflects the $C_\beta D$ covalent axis by just 4° (see Fig. 5). The intersection of the $C_\beta D$ curve with the previously determined value of θ' (162°) yields two possible solutions for χ_1', 165° and 188°. The χ_1 value for the dominant conformer is, therefore, either 161° or 184°.

In Fig. 8 solutions to θ' and ϕ' angles are also presented for the $C_\beta C_{\gamma 1}$ and $C_\beta C_{\gamma 2}$ bonds. Because of the greater extent of motional averaging for the methyl deuterons and the small quadrupole splitting these plots do not restrict the θ' angles

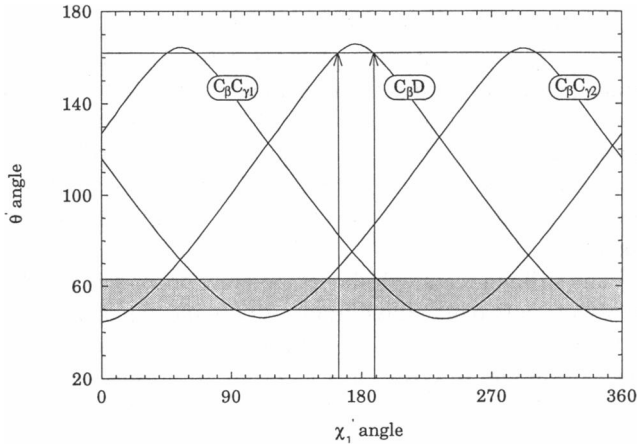

FIGURE 9 The θ' angles were calculated by rotating the χ_1' angles for the ν_{zz}(A3S) axes of $C_\beta D$, $C_\beta C_{\gamma 1}$, and $C_\beta C_{\gamma 2}$ deuterons over 360° in 1° increments. The orientation of the $C_\alpha C_\beta$ axis was shown to be 105°, close to the experimentally determined value of 100° (Ketchem et al., 1993). The intersect of the experimentally determined θ' value of 162° with the $C_\beta D$ line yields two possible χ_1' angles, 165° and 188°. The intersect of the θ' region with the $C_\beta C_{\gamma 1}$ line and the χ_1' angles defined above yields a unique χ_1' solution of 188°. The intersect of the $C_\beta C_{\gamma 2}$ line with the χ_1' value of 188° is consistent with the θ' range in Fig. 8.

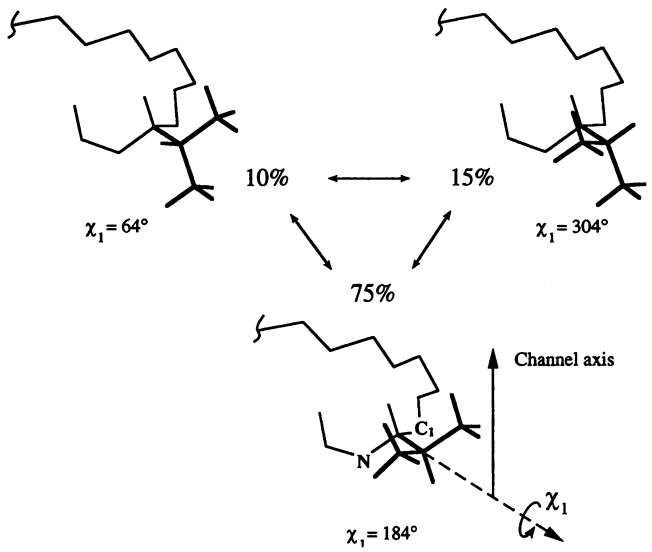

FIGURE 10 The rotameric states and their population distribution for the Val_1 gramicidin A site.

as substantially as in Fig. 8 *A*. However, the potential range of θ' between 49° and 63° is shown in Fig. 9 as a cross-hatched region. Only one of the χ_1' angles described above is consistent with the γ_1 methyl data and, therefore, χ_1' is uniquely defined as 188,° and χ_1 as 184°. Furthermore, the χ_1' angle of 188° yields an 87° θ' angle for $C_\beta C_{\gamma 2}$, which is well within the range described in Fig. 8 *C*. In Fig. 10 χ_1 of 184° is shown for the dominant conformer and χ_1 values of 304° and 64° for the second most common and least populated conformers, respectively.

The temperature dependence of the methyl quadrupole splittings have been observed previously (Killian et al., 1992) and is confirmed here (Fig. 7), although the range of temperature over which the splitting is sensitive is somewhat different. The gel to liquid crystalline phase transition is centered at 28°C, and at this high molar ratio of gramicidin the transition is very broad (approximately ±5°C at half-height on a DSC trace; Nicholson et al., 1987). Consequently, the temperature dependence observed here appears to be associated with the phase transition. In Killian et al. (1992), the reported temperatures were a few degrees higher for similar spectra.

The striking feature of the temperature dependence is that it affects only one methyl group. A possible explanation exists in that the θ' angle is 87° for $C_\beta C_{\gamma 2}$ and 63° for $C_\beta C_{\gamma 1}$. The sensitivity of $\cos^2\theta'$ is a factor of 10 greater for $C_\beta C_{\gamma 1}$ than for $C_\beta C_{\gamma 2}$; consequently, a small change in the orientation of the motional axis could have virtually no effect on the quadrupole splitting for $C_\beta C_{\gamma 2}$ while having a very significant effect on $C_\beta C_{\gamma 1}$. Alternatively, a small change in population distribution for the χ_1 jump motion could be the cause for such a temperature effect.

The separation and quantification of dynamics and structural influences on solid state NMR spectra are difficult to achieve. Through the observation of both powder pattern and oriented spectra, it has been possible to achieve a detailed description of both for a polypeptide side-chain within a lipid bilayer. In so doing it has not been necessary to involve eclipsed torsion angles or distortions in tetrahedral geometry (Killian et al., 1992). In fact, the dominant conformers for the Val-1 site are identified as the most common valine rotameric state from protein structures. Furthermore, the distribution among the rotameric states that describes the large amplitude dynamics about χ_1 appears to be consistent with the distribution of observed valine conformations from the Protein Data Bank.

It is clearly shown that the three-state jumps for valine occur under a variety of conditions from above and below the phase transition temperature of a lipid bilayer to dehydrated powders. This suggests that the distribution of conformational substates for this valine side-chain in contact with the lipid environment is largely independent of this environment. It remains to be seen whether this is a general property of valine of even aliphatic residues for gramicidin in lipid bilayers. Although the substate distribution is approximately constant, the residence time between jumps is dependent upon the phase of the lipid environment. Moreover, it is known that the conductance rate for the gramicidin channel is dependent on the phase of the lipid environment (Krasne et al., 1971). How the effects of the lipid phase are mediated by the channel to effect the conductance is not known, but it is possible that side-chain dynamics will play an important role in this process.

We are indebted to J. Vaughn, R. Rosanske, and T. Gedris of the NMR Facility and to U. Goli and H. Henricks of the Bioanalytical Synthesis and Services Facility for their expertise and help in this effort. T.A. Cross gratefully acknowledges National Science Foundation support from the Biophysics Program DMB 90–05938 and MCB 93–17111.

REFERENCES

Andersen, O. S., D. B. Sawyer, and R. E. Koeppe II. 1992. Modulation of Channel Function by the Host Bilayer in Biomembrane Structure & Function—The State of the Art. B. P. Gaber and K. R. K. Easwaran, editors. Adenine Press. 227–243.

Batchelder, L. S., C. E. Sullivan, L. W. Jelinski, and D. A. Torchia. 1982. Characterization of leucine sidechain reorientation in collagen-fibrils by solid-state ^2H NMR. *Proc. Natl. Acad. Sci. USA*. 79:386–389.

Beshah, K., and R. G. Griffin. 1989. Deuterium quadrupole echo NMR study of methyl group dynamics in *N*-Acetyl-DL-(γ-d_6)-valine. *J. Magn. Reson.* 84:268–274.

Beshah, K., E. T. Olejniczak, and R. G. Griffin. 1987. Deuterium NMR study of methyl group dynamics in L-alanine. *J. Chem. Phys.* 86: 4730–4736.

Colnago, L. A., K. G. Valentime, and S. J. Opella. 1987. Dynamics of fd coat protein in the bacteriophage. *Biochemistry*. 26:847–854.

Davis, J. H., K. R. Jeffrey, M. Bloom, M. I. Valic, and T. P. Higgs. 1976. Quadrupolar echo deuteron magnetic resonance spectroscopy in ordered hydrocarbon chains. *Chem. Phys. Lett.* 42:390–394.

Fields, G. B., C. G. Fields, J. Petefish, H. E. Van Wart, and T. A. Cross. 1988. Solid-phase peptide synthesis and solid-state NMR spectroscopy of [Ala^3-^{15}N][Val^1]gramicidin A. *Proc. Natl. Acad. Sci. USA*. 85: 1384–1388.

Fields C. G., G. B. Fields, R. L. Noble, and T. A. Cross. 1989. Solid phase synthesis of ^{15}N gramicidin A, B, and C and high performance liquid chromatographic purification. *Int. J. Pep. Protein Res.* 33: 298–303.

Greenfield, M. S., A. D. Ronemus, R. L. Vold, R. R. Vold, P. D. Ellis, and T. E. Raidy. 1987. Deuterium quadrupole-echo NMR spectroscopy. III. Practical aspects of lineshape calculations for multiaxis rotational processes. *J. Magn. Reson.* 72:89–107.

Huang, T. H., R. P. Skarjune, R. J. Wittebort, R. G. Griffin, and E. Oldfield. 1980. Restricted rotational isomerization in polymethylene chains. *J. Am. Chem. Soc.* 102:7377–7379.

Ketchem, R. R., W. Hu, and T. A. Cross. 1993. An experimental structure determination of the polypeptide backbone and the indole sidechains of the Gramicidin A channel conformation. *Science.* 261:1457–1460.

Keniry, M. A., A. Kintanar, R. L. Smith, H. S. Gutowsky, and E. Oldfield. 1984. Nuclear magnetic resonance studies of amino acids and proteins. Deuterium nuclear magnetic resonance relaxation of deuteriomethyl-labeled amino acids in crystals and in *Halobacterium halobium* and *Escherichia coli* cell membranes. Biochemistry. 23: 288–298.

Keniry, M. A., T. M. Rothgeb, R. L. Smith, H. S. Gutowsky, and E. Oldfield. 1983. Nuclear magnetic resonance studies of amino acids and proteins. Sidechain mobility of methionine in the crystalline amino acid and in crystalline sperm whale (*Physeter catodon*) myoglobin. *Biochemistry.* 22:1917–1926.

Kinsey, R. A., A. Kintanar, M.-D. Tsai, R. L. Smith, N. Janes, and E. Oldfield. 1981. First observation of amino acid side chain dynamics in membrane proteins using high field deuterium nuclear magnetic resonance spectroscopy. *J. Biol. Chem.* 256:4146–4149.

Killian, J. A. 1992. Gramicidin and Gramicidin-Lipid Interactions. *Biochim. Biophys. Acta.* 1113:391–425.

Killian, J. A., M. J. Taylor, and R. E. Koeppe. 1992. Orientation of the valine-1 side chain of the gramicidin transmembrane channel and implications for channel functioning. A ^{2}H NMR study. *Biochemistry.* 31: 11283–11290.

Krasne, S., G. Eisenman, and G. Szabo. 1971. Freezing and melting of lipid bilayers and mode of action of nonactin, valinomycin and gramicidin. *Science.* 174:412–415.

Lee, C. W. B., J. S. Waugh, and R. G. Griffin. 1986. Solid-state NMR study of trehalose/1,2-dipalmitoyl-sn-phosphatidylcholine interactions. *Biochemistry.* 25:3737–3742.

Lee, K.-C., W. Hu, and T. A. Cross. 1993. ^{2}H NMR determination of the global correlation time of the gramicidin channel in a lipid bilayer. *Biophys. J.* 65:1162–1167.

Leo, G. C., L. A. Colnago, K. G. Valentime, and S. J. Opella. 1987. Dynamics of fd coat protein in lipid bilayers. *Biochemistry.* 26:854–862.

Mai, W., W. Hu, C. Wang, and T. A. Cross.1993. Orientational constraints as three dimensional structural constraints from chemical shift anisotropy: the polypeptide backbone of gramicidin A in a lipid bilayer. *J. Protein Sci.* 2:532–542.

Nicholson, L. K., F. Moll, T. E. Mixon, P. V. LoGrasso, J. C. Lay, and T. A. Cross. 1987. Solid state ^{15}N NMR of oriented lipid bilayer bound gramicidin A. *Biochemistry.* 26:6621–6626.

Nicholson, L. K., Q. Teng, and T. A. Cross. 1991. Solid-state nuclear magnetic resonance derived model for dynamics in the polypeptide backbone of the gramicidin A channel. *J. Mol. Biol.* 218:621–637.

North, C. L. 1993. Ph. D. Dissertation.

North, C. L., and T. A. Cross. 1993. Analysis of polypeptides backbone T_1 relaxation data using an experimentally derived model. *J. Magn. Reson.* 101(B):35–43.

Prosser, R. S, J. H. Davis, F. W. Dahlquist, and M. A. Lindorfer. 1991. ^{2}H Nuclear Magnetic Resonance of the Gramicidin A Backbone in a Phospholipid Bilayer. *Biochemistry.* 30:4687–4696.

Wallace, B. A. 1990. Gramicidin Channels and Pores. *Annu. Rev. Biophys. Biophys. Chem.* 19:127–157.